

## Quasifree expansion picture of break-up events: An analysis of ionizing systems

L. F. Errea, L. Méndez, B. Pons,\* A. Riera, and I. Sevilla

*Laboratorio de Física Atómica Molecular en Plasmas de Fusión Nuclear, asociado al CIEMAT, Departamento de Química C-IX, Universidad Autónoma de Madrid, 28049 Madrid, Spain*

(Received 19 April 2002; published 28 February 2003)

We derive some general characteristics of the wave function representing a break-up event, in the asymptotic region. They have a strong bearing on the validity of some classical pictures, on the correlation between spatial and momentum variables that develops in the course of the dissociation process and on stringent requirements on the basis sets that are employed to approximate the wave function. Although other calculations are mentioned to underline the generality of our reasonings, we restrict most of the presentation, and all of the illustrations, to the case of ionization.

DOI: 10.1103/PhysRevA.67.022716

PACS number(s): 34.10.+x, 34.50.Fa

### I. INTRODUCTION

The description of break-up events, such as ionization or dissociation induced by dynamical processes or photon impact, involves the solution of the corresponding time-dependent Schrödinger equation. This requires an accurate representation of the electronic and/or nuclear continua, and specific algorithms have been derived, based on either lattice representations [1,2] or expansions in terms of “effectively” complete basis sets [3–5].

In the present work we report some important, and very general, requirements on those algorithms in order to represent the dissociating wave function in the asymptotic region, and that follow directly from the mechanism, rather than from empirical findings. For the sake of clarity and cogency of our analysis, we shall explicitly deal with, and confine our illustrations to, the specific case of ionization in atomic collisions, although calculations on photodissociation will be mentioned at the end of the paper. Our main points will be highlighted to clarify the presentation.

### II. THE ASYMPTOTIC MECHANISM AND THE “EXPLOSION” PHASE

A classical treatment of ionization [6] showed that the dominant mechanism is a relatively fast process whereby an electron becomes unbound, followed by a quasi-free expansion of the electron cloud. Hence, even in the case of long-range Coulomb forces this limits the role of interfragment interactions to that of secondary, though important, post collisional effects. The mechanism was then heuristically related to the (explosion) phase of the wave function in a quantal treatment. Although semiclassical calculations [4,5,7] confirmed this relation, the derivation of the phase was empirical, even though the same type of expansion phases appear (e.g., Refs. [8,9]) as a mathematical tool in the use of scaling methods.

Here we start by showing that by using the momentum representation the phase follows from the mechanism, and

allows to directly and unambiguously check on the relevance of the force-free picture, while pointing to its generality for most break-up process. It suffices to assume that after the electron becomes liberated, and for a (sizeable) domain of  $\mathbf{p}$  values, the main features of the ionizing wave function  $\phi(\mathbf{p},t) = |\phi(\mathbf{p},t)|\exp[i\alpha(\mathbf{p},t)]$  are given by the solution of the field-free Schrödinger equation

$$\left(\frac{p^2}{2m} - i\hbar \frac{\partial}{\partial t}\right)\phi(\mathbf{p},t) = 0 \quad (1)$$

with the “initial” condition at the (average) time of ionization  $t = t_0$ ,

$$\phi(\mathbf{p},t_0) = |\phi(\mathbf{p})|\exp[i\alpha_0(\mathbf{p})]. \quad (2)$$

This solution takes the form for  $t \geq t_0$ ,

$$\phi(\mathbf{p},t) = \phi(\mathbf{p},t_0)\exp\left[-\frac{i}{2m\hbar}p^2(t-t_0)\right], \quad (3)$$

so that we have  $|\phi(\mathbf{p},t)| = |\phi(\mathbf{p})|$ , whose specific form depends on the details of the ionization process for  $t < t_0$ , and

$$\alpha(\mathbf{p},t) = \alpha_0(\mathbf{p}) - \frac{1}{2m\hbar}p^2(t-t_0). \quad (4)$$

To check this, we have chosen the usual benchmark of  $\text{He}^{2+} + \text{H}(1s)$  collisions. We have selected a representative nuclear trajectory with impact parameter  $b = 1.2$  a.u. and a nuclear velocity  $v = 3$  a.u., for which the physical mechanism of soft-electron emission was shown in Ref. [7]. As in that reference, the spatial wave function was calculated with the method of Pons [4], using a target-centered expansion in terms of all spherical Bessel  $j_l(kr)$  functions such that  $j_l(kr_{max}) = 0$  with  $r_{max} = 100$  a.u.,  $0 \leq l \leq 3$  and  $0 \leq k \leq 3$  a.u.; all spherical harmonics were included up to  $m = 2$  and the momentum wave function was obtained by the fast Fourier transform method.

Figure 1 displays the values of the radial component of  $\nabla_p \alpha$  as a function of  $p$  for  $t = 20/3$  and  $50/3$  a.u. Comparison to the straight line  $-pt/m\hbar$  ( $= -pt$  in atomic units) shows that the free-expansion behavior of Eq. (4) is fulfilled, with  $t_0 \approx 0$ , and that  $\nabla_p \alpha_0$  can be neglected for sufficiently large  $p$

\*Permanent address: CELIA, UMR 5107 du CNRS, Université de Bordeaux-I, 351 Cours de la Libération, F-33405 Talence, France.

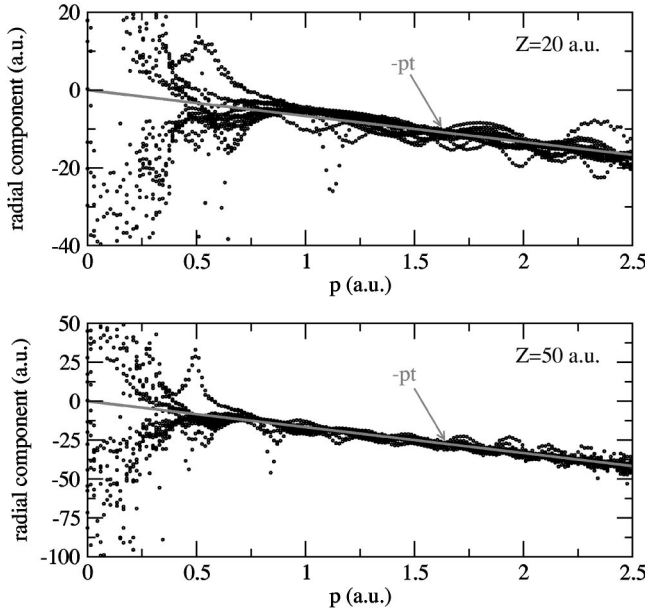


FIG. 1. Radial component of  $\nabla_{\mathbf{p}}\alpha(\mathbf{p},t)$  with  $\alpha(\mathbf{p},t)$  the phase of the momentum ionizing wave function for  $t=20/3$  and  $50/3$  a.u., as a function of the modulus  $p$  and for fixed values of the angular coordinates ( $\theta_p \in [0, \pi/4, \pi/2, \dots, \pi]$ ,  $\phi_p \in [0, \pi/4, \pi/2, \dots, 2\pi]$ ). The straight line  $-pt$  denotes the free-expansion behavior of Eq. (4). For the sake of a clearer comparison with the straight line  $-pt$ , we present this illustration for discrete  $p$  values rather than continuous curves.

(say,  $p > p_H$ ); we shall return to the value of  $p_H$  later on. The corresponding angular components of  $\nabla_{\mathbf{p}}\alpha$  are very small, and not shown for conciseness. In order to not restrict our attention to close-coupling approaches, we have checked that the same behavior also holds for the standard, impact-parameter first Born approximation [10].

We now consider the corresponding spatial wave function  $\psi(\mathbf{r},t) = |\psi(\mathbf{r},t)|\exp[iS(\mathbf{r},t)/\hbar]$ . This fulfills the force-free equation, so that the polar phase  $S$  satisfies

$$\frac{\partial S}{\partial t} + \frac{(\nabla S)^2}{2m} = \frac{\hbar^2}{2m} \frac{\nabla^2 |\psi|}{|\psi|}. \quad (5)$$

Both the modulus and phase of spatial and momentum wave functions can be closely related for  $t \gg t_0$  [11] starting from

$$\psi(\mathbf{r},t) = \frac{1}{(2\pi\hbar)^{3/2}} \int \exp\left(\frac{i}{\hbar} \left[ \mathbf{p} \cdot \mathbf{r} - \frac{p^2(t-t_0)}{2m} \right]\right) \phi(\mathbf{p},t_0) d\mathbf{p}, \quad (6)$$

and using the usual stationary phase approximation for the integral,

$$\psi(\mathbf{r},t) \sim \left(\frac{m}{t-t_0}\right)^{3/2} \phi(\mathbf{p}_s, t_0) \exp\left(i \left[ -\frac{3\pi}{4} + \frac{1}{2\hbar} p_s^2 (t-t_0) \right]\right) \quad (7)$$

with the point of stationary phase  $\mathbf{p}_s = m\mathbf{r}/(t-t_0)$ . Substitution of Eq. (2) in Eq. (7) yields

$$\psi(\mathbf{r},t) \sim |\psi(\mathbf{r},t)| \exp\left(i \left[ -\frac{3\pi}{4} + \alpha_0 \left( \frac{m\mathbf{r}}{t-t_0} \right) + \frac{mr^2}{2\hbar(t-t_0)} \right]\right) \quad (8)$$

with  $|\psi(\mathbf{r},t)| = (m/(t-t_0))^{3/2} |\phi(\mathbf{p}_s)|$ , and  $S(\mathbf{r},t)$  takes what is essentially the form of Ref. [6], which is now obtained as a consequence of the free-expansion picture, rather than working by analogy.

### III. VALIDITY OF CLASSICAL PICTURES

We next show that the relevance of classical trajectory Monte Carlo (CTMC) treatments follows from Eq. (8). First, one can often neglect  $\nabla \alpha_0[m\mathbf{r}/(t-t_0)]$  in the calculation of  $\nabla S$ , as may be expected from Fig. 1 and from Ref. [7]. Then,  $S$  fulfills the field-free Hamilton-Jacobi equation with a classical velocity  $\mathbf{v}_C = \hbar \nabla S/m$  that is identical to the best estimate of the quantal velocity  $\mathbf{j}(\mathbf{r},t)/m|\psi(\mathbf{r},t)|^2$ , obtained from Eq. (8). Since this is also obtained from Eq. (5) in the classical  $\hbar/m \rightarrow 0$  limit (i.e.,  $|\nabla^2|\psi| \ll |\psi|$  in atomic units), there results a justification of classical calculations for  $t > t_0$ . In particular, the arrow diagrams of Refs. [6,7] may be considered as snapshots of a “geometrical optics” approximation for the wave motion of the ionized electron, which differs from usual limiting procedure [12] in that it does not require that the spread of the wave packet be smaller than its width. We note that the justification for the CTMC calculations for  $t < t_0$  also differs [7] from the standard semiclassical limit (which, as reasoned in Ref. [13], is inapplicable to soft-electron emission), and hinges on the way the statistical distribution is generated, and on the specific nature of the Coulomb interaction.

The classical analogy can in turn be employed to provide estimates of the  $p > p_H$  and  $r > r_H$  domains where Eqs. (3) and (8) can be expected to hold. We can take  $p_H$  and  $r_H$  as the smallest values fulfilling  $\mathbf{p}_s = m\mathbf{r}/(t-t_0)$  and such that the electron is unbound [14] with respect to the target field  $p_H^2/2m - e^2/r_H = 0$ . This yields the conditions

$$p > p_H = \left(\frac{2e^2 m^2}{t-t_0}\right)^{1/3}; \quad r > r_H = \left[\frac{2e^2(t-t_0)^2}{m}\right]^{1/3}, \quad (9)$$

which gives, in particular,  $p > 0.67, 0.49$  a.u. for  $t = 20/3$  and  $50/3$  a.u., respectively, in agreement with Fig. 1; we find a similar accordance for the spatial wave function.

### IV. CORRELATION BETWEEN SPATIAL AND MOMENTUM VARIABLES

Since we should have from Eq. (7) that  $|\psi(\mathbf{r},t)| \sim [m/(t-t_0)]^{3/2} |\phi(m\mathbf{r}/(t-t_0), t)|$ , spatial and momentum representations are directly related. We illustrate this by displaying in Fig. 2 the one-dimensional Cartesian (scaled) spatial and momentum densities, obtained by integrating  $|\psi(\mathbf{r},t)|^2$  and  $|\phi(\mathbf{p},t)|^2$ , respectively, over the remaining variables. To describe these densities, we neglect  $\alpha_0(\mathbf{p})$ , and fit them by means of normal distributions  $g(p_\gamma) = \exp(-p_\gamma^2/4\sigma_p^2)/[(2\pi)^{1/4}\sigma_p^{1/2}]$ :

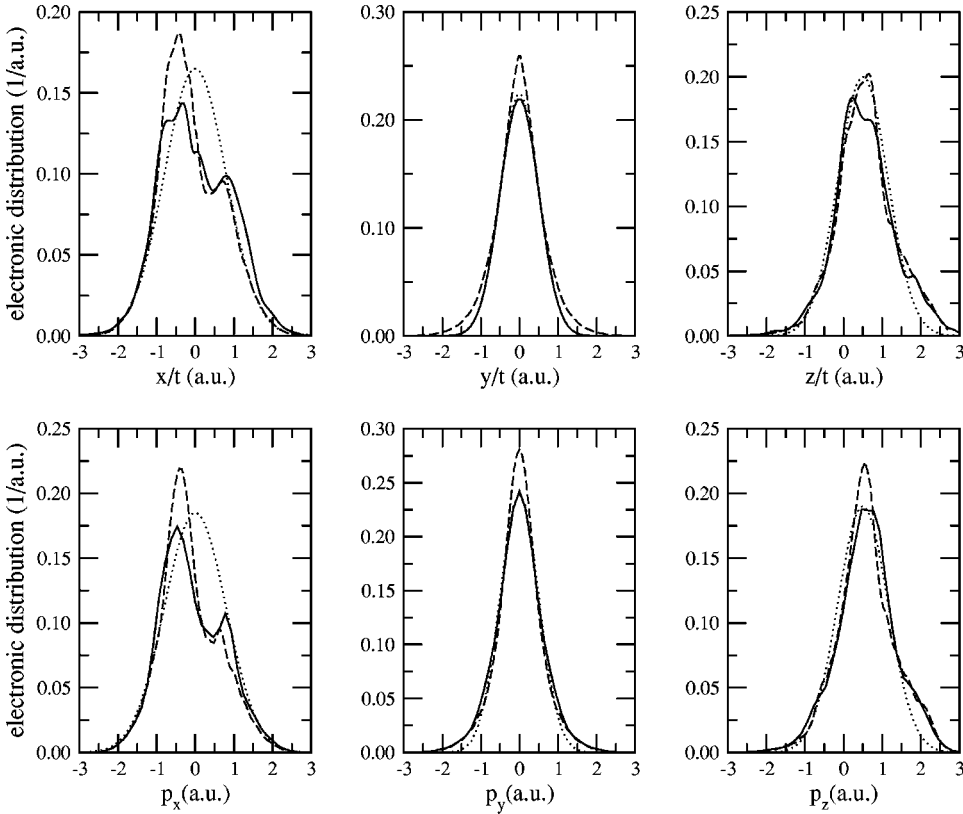


FIG. 2. One-dimensional spatial (top) and momentum (bottom) distributions of ejected electrons, for  $t=20/3$  (solid line) and  $50/3$  (dashed line) a.u. The dotted lines correspond to the fits by means of normal Gaussian distributions (see text) with  $\sigma_{p_x}=0.8$  a.u.,  $\sigma_{p_y}=0.4$  a.u., and  $\sigma_{p_z}=0.65$  a.u. In the laboratory-fixed reference frame,  $\mathbf{r}=(x,y,z)$  and  $\mathbf{p}=(p_x,p_y,p_z)$ , with  $\hat{\mathbf{x}}=\widehat{\mathbf{p}}_{\mathbf{x}}=\hat{\mathbf{b}}$ ,  $\hat{\mathbf{z}}=\widehat{\mathbf{p}}_{\mathbf{z}}=\hat{\mathbf{v}}$ , and  $\hat{\mathbf{y}}$  and  $\widehat{\mathbf{p}}_{\mathbf{y}}$  perpendicular to the collision ( $\hat{\mathbf{v}},\hat{\mathbf{b}}$ ) plane.

$$\phi(\mathbf{p},t) \approx \|\phi\| g(p_x)g(p_y)g(p_z) \exp\left(-\frac{ip^2(t-t_0)}{2m\hbar}\right), \quad (10)$$

where  $\sigma_{p_\gamma}$  is a measure of the uncertainty of  $p_\gamma$  and  $\|\phi\|^2 = \|\phi(\mathbf{p},t_0)\|^2 = \|\psi\|^2$  is the ionization probability. The Fourier transform of Eq. (10) takes an analytical form that tends for  $t \gg t_0$  to the expression of Eq. (7). The relevance of the normal distributions can be gauged from Fig. 2; we see that the  $y, p_y$  distributions are practically normal, as may be expected from the accumulation of the ionizing density about the collision plane [13]. On the other hand, the fact that the ionized cloud is pulled towards the projectile [7] results in that the maximum of the  $p_z$  distribution is shifted to  $p_z = 0.5$  a.u.; also, the rotation of the ionized cloud [7] results in a more irregular  $p_x$  distribution. The same features hold for the scaled spatial densities (see Fig. 2).

We can examine the connection between spatial and momentum representations more closely by considering the corresponding Wigner distribution [15,16] that takes the form from Eq. (3)

$$W(\mathbf{r},\mathbf{p},t) = \frac{1}{(2\pi\hbar)^3} \int \exp\{-i\mathbf{q} \cdot [\mathbf{r} - \mathbf{p}(t-t_0)/m]/\hbar\} \times \phi(\mathbf{p} - \mathbf{q}/2, t_0) \phi^*(\mathbf{p} + \mathbf{q}/2, t_0) d\mathbf{q}. \quad (11)$$

It follows from the Riemann-Lebesgue lemma that  $W \rightarrow 0$  as  $t \rightarrow \infty$ , except when  $\mathbf{p} = m\mathbf{r}/(t-t_0)$ , in which case it remains constant in time. Hence, for large  $t$  values there develops an increasingly stronger correlation between spatial and mo-

mentum variables, such that the relative velocity between two portions of the ionizing cloud lies along the line joining them and is proportional to their separation; this is just as found in Ref. [6]. To illustrate this correlation property, we display in Fig. 3 the partial Wigner functions  $W_x, W_y, W_z$  for  $t = 20/3$  and  $50/3$  a.u., where  $W_\gamma(\gamma, p_\gamma, t)$  is obtained by integrating  $W(\mathbf{r}, \mathbf{p}, t)$  over the remaining coordinates. To analyze these functions, we use the normal approximation for the densities, by substituting Eq. (10) in Eq. (11),

$$W \approx \|\phi\|^2 f(x, p_x, t) f(y, p_y, t) f(z, p_z, t) f(\gamma, p_\gamma, t) = (\pi\hbar)^{-1} \exp\left(-\frac{p_\gamma^2}{2\sigma_{p_\gamma}^2} - \frac{2\sigma_{p_\gamma}^2}{m^2\hbar^2} [m\gamma - p_\gamma(t-t_0)]^2\right). \quad (12)$$

As  $t \rightarrow \infty$ , the correlation coefficient of both sets of bivariate distributions tends to unity, and the distributions degenerate into ‘‘sheets’’ in phase space (see Fig. 3), just as the classical distribution function [11],

$$W \rightarrow (t-t_0)^3 m^3 (\hbar/\pi)^{3/2} \sigma_{p_x} \sigma_{p_y} \sigma_{p_z} \|\phi\|^2 \times \exp\left(-\frac{p_x^2}{2\sigma_{p_x}^2} - \frac{p_y^2}{2\sigma_{p_y}^2} - \frac{p_z^2}{2\sigma_{p_z}^2}\right) \delta\left(\mathbf{p} - \frac{m\mathbf{r}}{t-t_0}\right). \quad (13)$$

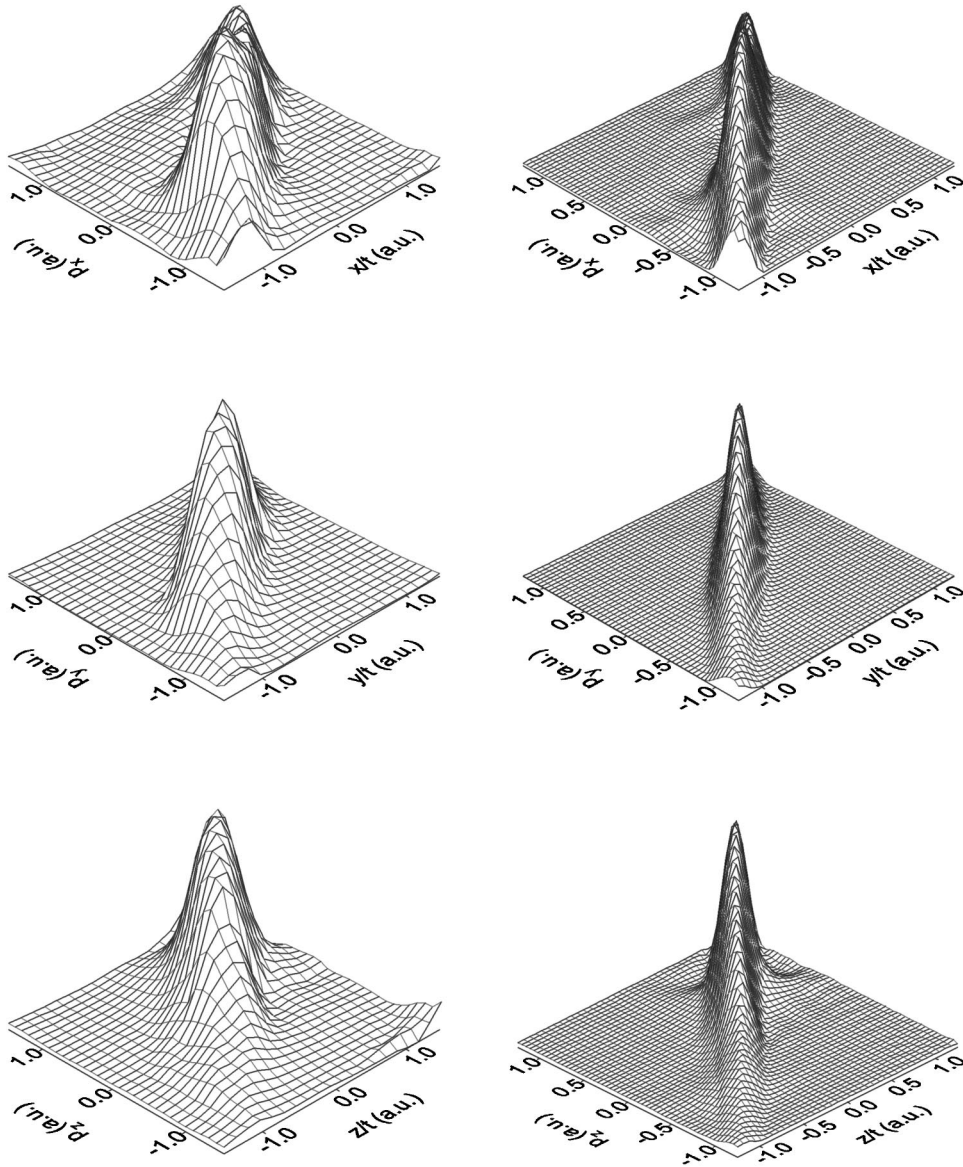


FIG. 3. Partial Wigner distributions  $W_\gamma(\gamma, p_\gamma, t)$  with  $\gamma \equiv \{x, y, z\}$ , for  $t=20/3$  (left column) and  $50/3$  (right column) a.u.

## V. REQUIREMENTS ON BASIS SETS

A major consequence of our analysis is the condition that numerical treatments should be able to describe both the expansion of the spatial wave function and the “explosion” phase  $\exp(iS/\hbar)$  of Eq. (8). It should be noted, in this respect, that we do not necessarily advocate that basis functions should expand in time or explicitly contain the phase, only that they can be able to reproduce these features. This is a nontrivial requirement. For instance, in the case of ionization the failure of molecular methods to describe the phase results [17] in an unphysical trapping of the ionizing flux, hence in inaccurate wave functions (though not necessarily in inaccurate cross sections).

A corresponding liability [4] holds for the usual atomic basis sets of Slater-type orbitals (STO’s), Sturmian, or Gaussian orbitals. We display in Fig. 4 the values of the ionizing probability  $\|\psi\|^2$  along our selected nuclear trajectory, and we compare it to  $\|P^{1C-STO}\psi\|^2$ , where  $P^{1C-STO}$  is the projector onto the manifold spanned by a set of even-

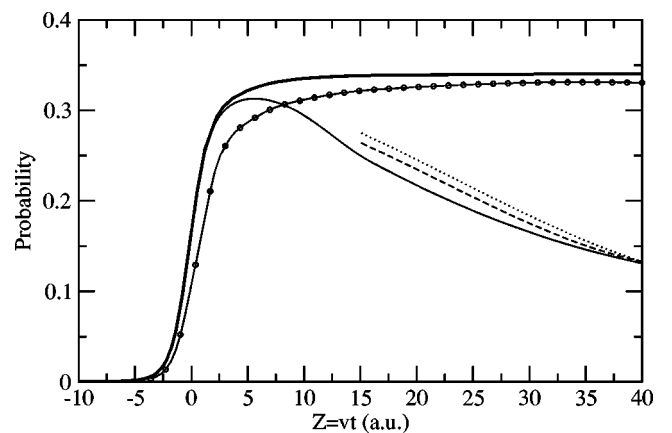


FIG. 4. Ionization probability  $\|\psi\|^2$  (thick line) compared to values obtained from projections of the ionizing wave function onto various types of close-coupling sets, as defined in text:  $\|P^{1C-STO}\psi\|^2$  (thin line),  $\|P^{2C-STO}\psi\|^2$  (dashed line),  $\|P^{2C-PWTF}\psi\|^2$  (dotted line),  $\|P^{1C-EEF}\psi\|^2$  (dot-connected line).

tempered STO's  $r^l e^{-\alpha_n r} Y_{lm}(\hat{\mathbf{r}})$  centered at the target nucleus, with  $\alpha_n = 0.001(1.3)^n$  and  $0 \leq n \leq 39$ . While this large basis is capable of describing the ionization process taking place at short  $R$ , its quality deteriorates at large distances. Use of a two-center basis ( $P^{2C-STO}$ ), that consists of the same STO set located on both target and projectile centres, or modification of these basis functions with plane-wave translation factors [18] ( $P^{2C-PWTF}$ ), does not significantly improve the situation. On the other hand, multiplication of the STO by the explosion factor  $\exp(ivr^2/2R) \approx \exp(ir^2/2t)$  (in atomic units), yielding  $P^{1C-EEF}$ , strikingly improves the quality of the single-center basis: this unambiguously proves that the failure of the usual (atomic and molecular) close-coupling expansions in describing the ionization process in the asymptotic region is due to their inability to reproduce the free-expansion phase.

## VI. GENERALITY OF THE PRESENT FINDINGS

We now consider the limitations of our analysis for general break-up events. Obviously, how large  $t$  must be for our reasoning to apply depends on the particular physical situation. It would never apply for a hypothetical state possessing a sharp value for the momentum conjugate to the dissociation coordinate, such as represented by  $\delta(p - p_d) Y_{lm}(\theta_p, \varphi_p)$ ; then the phase of the momentum wave function becomes  $\exp(-ip_d^2 t/2m\hbar) = \exp(-iE_d t/\hbar)$ , with  $E_d$

being the fragmentation energy. The spatial wave function is then written in terms of spherical waves in the coordinate of dissociation, without an expansion phase. However, in practical situations there is always a sizeable momentum spread  $\sigma_p$  and an energy spread  $\sigma_E$ , which are determined by the dynamics of the process or by the linewidth of the radiation. Then the condition for the stationary phase approximation (7) to apply is  $t - t_0 \gg \hbar/\sigma_E$ . In turn, this corresponds to a domain of interfragment distances that depends on the velocity of separation.

In particular, in our calculations on photodissociation events we found that in the absence of Coulomb forces the quasi-free expansion mechanism applies from a few atomic units of internuclear separation onwards; in turn, this corresponds to  $t$  values of the order of hundreds of a.u., because of the small velocities involved. Explicitly, calculations were carried out for  $H_2^+$  dissociation by strong ( $I = 10^{13}$  W/cm<sup>2</sup>) and short (FWHM  $\tau = 15$  fs) laser pulses, within the two electronic states Born Oppenheimer approximation [19], and the vibrational basis consisted of a set of spherical Bessel functions  $j_0(kR)$  similar to that of the examples given in the present paper.

## ACKNOWLEDGMENTS

This work was partially supported by DGICYT Project Nos. SFM2000-0025 and FTN2000-0911.

- 
- [1] A.D. Bandrauk and H. Zhong Lu, Phys. Rev. A **62**, 053406 (2000); D. Dundas *et al.*, J. Phys. B **33**, 3261 (2000).
- [2] D.R. Schultz *et al.*, Phys. Rev. A **65**, 052722 (2002); M. Chasid and M. Horbatsch, *ibid.* **66**, 012714 (2002).
- [3] H. Bachau *et al.*, Rep. Prog. Phys. **64**, 1815 (2001).
- [4] B. Pons, Phys. Rev. Lett. **84**, 4569 (2000); Phys. Rev. A **63**, 012704 (2001); **64**, 019904 (2001).
- [5] E.Y. Sidky and C.D. Lin, Phys. Rev. A **65**, 012711 (2001).
- [6] C. Illescas and A. Riera, Phys. Rev. Lett. **76**, 1043 (1998).
- [7] C. Illescas *et al.*, Phys. Rev. A **63**, 062722 (2001).
- [8] J.P. Grozdanov and E.A. Solov'ev, Eur. Phys. J. D **6**, 13 (1999).
- [9] E.Y. Sidky and B.D. Esry, Phys. Rev. Lett. **85**, 5086 (2000).
- [10] M.R.C. McDowell and J.P. Coleman, *Introduction to the Theory of Ion-atom Collisions* (North-Holland, Amsterdam, 1970).
- [11] A. Riera, Comments Mod. Phys. **1**, 131 (1999).
- [12] A. Messiah, *Quantum Mechanics* (North-Holland, Amsterdam, 1961).
- [13] N. Stolterfoht *et al.*, *Electron Emission in Heavy Ion-Atom Collisions* (Springer-Verlag, Berlin, 1997).
- [14] E.Y. Sidky *et al.*, Phys. Rev. Lett. **85**, 1634 (2000).
- [15] E.P. Wigner, Phys. Rev. **40**, 749 (1932).
- [16] H.W. Lee, Phys. Rep. **259**, 147 (1995).
- [17] L.F. Errea *et al.*, Phys. Rev. A **65**, 022711 (2002).
- [18] D.R. Bates and R. McCarroll, Proc. R. Soc. London, Ser. A **245**, 175 (1958).
- [19] S. Geltman, J. Phys. B **32**, 2309 (1999).